Stratospheric water vapor from the Hunga Tonga – Hunga Ha'apai volcanic eruption deduced from COSMIC-2 radio occultation

William J. Randel[1,2], Benjamin R. Johnston[2], John J. Braun[2], Sergey Sokolovskiy[2], Holger Vömel[1], Aurelien Podglajen[3] and Bernard Legras[3]

[1] National Center for Atmospheric Research, Boulder, CO 80301

[2] COSMIC Program Office, University Corporation for Atmospheric Research, Boulder, CO 80301

[3] Laboratoire de Météorologie Dynamique (LMD-IPSL), UMR CNRS 8539, ENS-PSL, École Polytechnique, Sorbonne Université, Institut Pierre Simon Laplace, Paris, France

Abstract

The eruption of the Hunga Tonga – Hunga Ha'apai (HTHH) volcano on January 15, 2022 injected large amounts of water vapor directly into the stratosphere. While normal background levels of stratospheric water vapor are not detectable in radio occultation (RO) measurements, effects of the HTHH eruption are clearly observed as anomalous refractivity profiles from COSMIC-2, suggesting the possibility of detecting the HTHH water vapor signal. To separate temperature vs. water vapor effects on refractivity, we use co-located temperature observations from the Microwave Limb Sounder (MLS) to constrain a simplified water vapor retrieval. Our results show enhancements of water vapor up to ~1500-2300 ppmv in the stratosphere (~29-33 km) in the days following the HTHH eruption, with propagating patterns that follow the dispersing volcanic plume. The stratospheric water vapor profiles derived from RO are in reasonable agreement with limited radiosonde observations over Australia.

Key Points:

- Radio occultation measurements detect stratospheric water vapor from the 2022 Hunga Tonga volcanic eruption.
- Stratospheric water vapor amounts exceeding 1000 ppmv are observed near 30 km during the first week after the eruption.
- COSMIC-2 results quantify stratospheric water vapor amounts and volcanic plume evolution.

Plain Language Summary

The explosive eruption of the Hunga Tonga – Hunga Ha'apai (HTHH) volcano in January 2022 injected extreme amounts of water vapor directly into the stratosphere. While normal background levels of stratospheric water vapor are not detectable in radio occultation (RO) measurements, impacts of the HTHH eruption are so large that they are identified in COSMIC-2 RO measurements. We develop a simplified water vapor retrieval using COSMIC-2 data and co-located temperature measurements from the Microwave Limb Sounder, finding enhancements of water vapor above 1000 ppmv at altitudes near 30 km during the days following the HTHH eruption. The stratospheric water vapor profiles derived from RO are in reasonable agreement with limited radiosonde observations over Australia. These RO measurements provide novel quantification of the unprecedented water vapor amounts and the plume evolution during the first week after the HTHH eruption.

1. Introduction

The January 2020 explosive volcanic eruption of Hunga Tonga – Hunga Ha'apai (~20° S, 175° W; hereafter HTHH) injected large amounts of water vapor (H_2O) directly into the stratosphere. Measurements from operational radiosonde balloons over Australia in the first several days after the eruption show local H_2O mixing ratios above 1000 ppmv over altitudes ~25-30 km (the top of the balloon measurements; Sellitto et al, 2022; Vömel et al, 2022), compared to typical stratospheric background H_2O values of 5 ppmv. The isolated balloon measurements showed that the H_2O enhancements occurred in relatively thin ~1-2 km layers. Measurements from the Microwave Limb Sounder (MLS) instrument on the NASA Aura satellite show H_2O perturbations from HTHH that are unprecedented in the satellite data record, in terms of both altitude and magnitude (Millán et al, 2022). The MLS data show enhanced H_2O at altitudes up to 53 km immediately after the eruption (January 15), and maxima between ~25-35 km during the following few days (January 16-18). Maximum H_2O values in these MLS retrievals, which represent averages over ~3 km, was ~200-400 ppmv. However, the standard MLS retrievals are not designed for the anomalously high stratospheric H_2O values from HTHH, and many of these early retrievals did not pass the MLS quality screening criteria (Millán et al, 2022). The HTHH plume traveled westward and dispersed in the stratosphere, and MLS data show that local H_2O maxima decreased to ~50 ppmv by early February, and to ~10-20 ppmv by late March. The MLS retrievals are much better characterized for the lower H_2O values after late January. Anomalous high H_2O from HTHH persists in the stratosphere through boreal summer 2022 and has spread over much of the globe (Xu et al., 2022; Legras et al., 2022; Khaykin et al., 2022).

The objective of this paper is to explore the retrieval of the extreme stratospheric H_2O amounts from HTHH in the first week after the eruption using COSMIC-2 (C2) GNSS radio occultation (RO) data. RO measures the bending angle of radio waves propagating through the atmosphere, which is closely related to atmospheric refractivity (N), which in turn is dependent on temperature and moisture. Under normal conditions, H_2O makes virtually no contribution to N in the stratosphere and thus is not detectable by RO measurements. However, effects from HTHH are clearly observed as anomalous stratospheric N profiles from C2 that follow the HTHH plume during the first week after the eruption (shown below).

These anomalous N profiles can potentially be associated with both temperature and H_2O effects from the HTHH eruption, and we separate these influences by using independent temperatures from nearby MLS measurements. Our results include comparisons with the limited radiosonde H_2O measurements over Australia (up to ~30 km) to help evaluate the H_2O profiles derived from C2 measurements.

2. Data and Analyses

a) C2 GNSS-RO observations

By measuring the phase delay of radio waves from GNSS satellites as they slow and bend in Earth's atmosphere, profiles of bending angles and refractivity can be obtained (e.g. Anthes et al, 2008). At microwave frequencies in the troposphere and stratosphere, the refractivity varies due to contributions from the dry air and water vapor. Specifically, the atmospheric refractivity N can be related to atmospheric pressure p, temperature T, and water vapor partial pressure e (Smith and Weintraub 1953):

$$N = 77.6\left(\frac{p}{T}\right) + 3.73 \times 10^5\left(\frac{e}{T^2}\right) \quad (1)$$

In this study, we obtain level-2 C2 GNSS-RO profiles for January 2022 processed by the COSMIC Data Analysis and Archive Center (CDAAC) at the University Corporation for Atmospheric Research (UCAR). C2 is providing ~6000 profiles/day between ~40°N-40°S. We use the 'atmPrf' product, which provides refractivity and dry temperature (retrieved under the assumption of dry air) from near the surface up to ~60 km; data above 40 km are strongly influenced by climatology, and we focus on altitudes 25-35 km in this study. The profiles are quality controlled at CDACC by assigning 'bad' flags based on several metrics, including deviation from the climatology by a specific threshold. We note that a few C2 measurements intersect the early HTHH plume on January 15 and indicate large N anomalies, but these are flagged as 'bad' retrievals. These profiles are briefly discussed below and shown in the Supplement. The effective vertical resolution of RO soundings varies from ~200 m in the lower troposphere to ~1-2 km in the upper stratosphere (more details below) while the horizontal footprint (horizontal scale represented by a single observation) is ~200 km (e.g. Anthes et al, 2008).

At CDAAC, the neutral atmosphere profiles are retrieved in the geometric optics approximation above 20 km. In this approximation, the resolution is physically limited by the 1st Fresnel zone F_o [Kursinski et al., 1997] which depends on altitude and is about 1.4 km at 30 km. At CDAAC, data smoothing is performed using the Savitzky-Golay filter; details can be found in [Zeng et al., 2019]. The half-width of the filter response function used for the standard processing is $1.1F_0$ ~ 1.5 km at 30 km. Specifically for this study, we investigated the possibility of modifying the filtering in order to better resolve those N structures in the stratosphere induced by HTHH eruption. By modeling and testing we found that reducing the half-width of the response function by one-half, to 0.75 km at 30 km, results in improvement of the vertical resolution at 30 km without substantial increase of the effect of observational noise (mainly from the ionosphere), while further reduction increases the noise and creates artifacts in the profiles. Thus, C2 RO data used in this study were processed with twice increased vertical resolution compared to the standard retrieval.

b) MLS temperatures

MLS temperatures are retrieved using measured limb emission from atmospheric oxygen (O_2), and these data are not strongly influenced by the HTHH eruption. We use MLS temperature profiles based on the v4.2 retrieval (Livesey et al, 2022). MLS provides global sampling with approximately 3500 measurements per day. Temperature retrievals are provided on standard pressure levels; data extend from 261 hPa (~9 km) to above 1 hPa (~48 km, with an effective vertical resolution of 3-4 km over the main region of interest here (~30 km).

c) Radiosondes

We include comparisons with radiosonde measurements of stratospheric H_2O during the first few days after the HTHH eruption. These data are discussed in detail in Vömel et al (2022), based on measurements from the operational upper air network using the Vaisala RS41 radiosonde. These data can detect the large stratospheric H_2O from HTHH, and provide measurements up to ~ 30 km (depending on the balloon burst altitude of individual flights) with vertical resolution of ~100 m.

3. Results

a) RO sensitivity to stratospheric H_2O

N decreases strongly with altitude in the troposphere and stratosphere, and the H_2O term in (1) contributes little to *N* above the middle troposphere, where $H_2O < 100$ ppmv (e.g. Johnston et al, 2022). Sensitivity tests based on (1) can determine the magnitude of GNSS RO refractivity variations expected from isolated H_2O and temperature anomalies in the stratosphere. The sensitivity of *N* to an isolated large stratospheric H_2O perturbation (1000 ppmv anomaly at 30 km) is illustrated in Fig. 1, showing a positive *N* anomaly of ~3.5% compared to an unperturbed background. While this is a relatively small fractional *N* anomaly, it is not small compared to the observed *N* standard deviation in the stratosphere measured by C2, with typical values of 1% background levels (as shown in Fig. 1; these were calculated from the pre-volcanic C2 measurements in the vicinity of HTHH). Hence, an *N* anomaly due to a 1000 ppmv increase in H_2O is comparable to a (rare) positive 3-sigma C2 noise event. Figure 1 also shows the *N* anomaly associated with a local -8 K temperature perturbation at 30 km, which is similar (~3.5%) to the effect of 1000 ppmv H_2O. These calculations suggest that C2 RO measurements may be able to detect a large stratospheric H_2O perturbation on the order of 1000 ppmv, but that similar *N* signals can arise from large negative temperature anomalies.

b) C2 HTHH refractivity observations and H_2O retrievals

Based on the sensitivity calculations shown in Fig. 1, our analyses search for positive *N* anomalies in C2 data that are larger than 3-sigma. Anomalies are calculated as % differences from the non-volcanic background January average. Figure 2 shows the C2 daily sampling density in the region of the HTHH eruption on January 16, 17 and 18 (grey dots) along with the locations of local *N* anomalies with maximum values above 3-sigma over altitudes 25-35 km (colored symbols). The stratospheric plume from HTHH moved westward in the background stratospheric easterly winds (e.g. Sellitto et al, 2022; Millán et al, 2022), and the positive *N* anomalies >3-sigma in Fig. 2 track the plume movement downstream from the January 15 eruption. The altitudes of the *N* anomaly maxima for these days generally range from 27 to 33 km.

Examples of the vertical profiles of *N* anomalies for the cases identified on January 16 (Fig. 2a) are shown in Fig. 3a. As selected, each of the profiles has a maximum *N* anomaly above 3%, with several local maxima above 6%, and the observed profiles peak over altitudes ~29-33 km. The vertical thickness of the *N* anomaly profiles is ~2 km.

We calculate a simplified estimate of H_2O based on Eq. 1, incorporating C2 *N* observations and MLS temperatures as independent information, and using dry pressure *p* from the C2 atmPrf files. Specifically, for each profile we take the full C2 *N* profile (not anomalies) and find the nearest co-located MLS temperature profile (within 600 km and 6 hours). We then solve Eq. 1 for water vapor pressure *e* and convert to H_2O mixing ratio. Figure 3b shows the derived H_2O profiles on Jan. 16, with maximum H_2O values of ~1500-2300 ppmv over altitudes ~29-33 km; the altitude maxima for H_2O approximately match the *N* anomaly maxima in Fig. 3a. We note that these large H_2O amounts are below ice saturation with respect to the background stratospheric temperatures that increase with height (e.g. Sellitto et al., 2022; Vömel et al., 2022). Figures 3c-d show derived H_2O profile results for the following days, showing a decrease in the maximum H_2O amounts to ~1500-2000 ppmv on January 17 and ~1000 ppmv on January 18. The measured altitudes of the H_2O maxima also systematically decrease between January 16-18.

Analyses of the MLS temperatures show that there are not systematic temperature anomalies associated with the identified C2 *N* anomalies for the volcanic plume events (Fig. 4), so that the stratospheric RO N anomalies are arising primarily from enhanced H_2O. This statement is qualified by the lower vertical resolution of MLS temperatures (~4 km) compared to C2 retrievals (~1-2 km), in addition to imprecise co-locations of the MLS and C2 data. In contrast to the lack of temperature anomalies in the MLS data, temperatures derived from the C2 dry retrieval (atmPrf, neglecting the H_2O term in Eq. 1) show negative temperature anomalies up to -20 K (Fig. 4). These are likely spurious results related to the large positive *N* anomalies when not accounting for H_2O effects. As a note, we have also examined co-located temperatures from ERA5 reanalysis (Hersbach et al., 2020) and find small systematic temperature anomalies for the co-locations, similar to the MLS results in Fig. 4.

While the HTHH plume was over Australia on January 16-18, enhanced stratospheric H_2O was observed by operational radiosonde balloons (Sellitto et al, 2022; Vömel et al, 2022). H_2O profiles from these radiosonde data are shown in Fig. 3 overlain on the RO retrievals. Note that the top of the radiosonde measurements is near 30 km (depending on the individual balloon flights), so that direct comparisons with RO calculations focus on altitudes below 30 km. Also, the radiosonde profiles are not explicitly co-located with the C2 profiles but are intended to be representative of approximate H_2O magnitudes and altitudes in this region. The radiosonde-C2 comparisons in Figs. 3b-d show reasonable agreement over ~26-30 km in terms of H_2O magnitude (~1000-2000 ppmv) during these days. This agreement enhances confidence in the C2 H_2O retrievals, at least for the extreme maxima immediately following the eruption.

Regular westward propagation of the HTHH H_2O plume is detected by RO measurements over the first week after the eruption, as shown in Fig. 5a selected for profiles with derived H_2O values > 700 ppmv over 25-35 km. This behavior is in good agreement with the MLS H_2O retrievals shown in Millán et al (2022), who also demonstrate consistency with the background stratospheric easterly winds. Figure 5a also shows that while the enhanced H_2O values from HTHH clearly stand out, there are numerous additional events that are not coincident with the plume, and these likely represent noise in the C2 *N* profiles.

For the H_2O profiles identified in the HTHH plume (i.e., following the locus of westward propagating points in Fig. 5a), Figs. 5b-c show the derived plume height and maximum H_2O values. Results show highest H_2O magnitudes (~1500-2300 ppmv) and highest altitudes (~29-33 km) immediately after the eruption (January 16-17). The maximum H_2O magnitudes and altitudes generally decrease over time, although there are some isolated larger H_2O maxima over January 20-22 that could possibly be related to localized plume maxima identified in Legras et al (2022). Decreases in H_2O magnitude and altitude are consistent with observations from MLS (Millán et al, 2022) and radiosonde data (Vömel et al, 2022) following the eruption. The descent rate for the period January 18-23 in Fig. 5b is approximately 160 m/day, which is consistent with values estimated from radiosondes over the first zonal circumnavigation of the plume (~200m/d in Khaykin et al, 2022). We find less coherent variability in derived C2 H_2O amounts after ~January 24 (not shown). Given the

RO H_2O sensitivity inferred from Fig. 1 together with observed C2 noise levels, we expect that C2 will lose sensitivity to stratospheric H_2O amounts below ~700 ppmv (which corresponds to positive *N* anomalies ~2-sigma).

We have also investigated several C2 measurements that intersected the HTHH plume early after the eruption on January 15, and the associated *N* anomalies and retrieved H_2O amounts are shown in Fig. S1. The results show large positive *N* anomalies (~10-25%) and extreme H_2O values (~ 3,000 - 6,000 ppmv) over altitudes 30-40 km, and smaller maxima over 45-50 km. However, these retrieved *N* profiles are mostly classified as 'bad', and the reason is not simply understood because there are numerous potential causes. While we are less confident in these retrievals, the vertical structure is reasonable and the large H_2O values in Fig. S1are still below ice saturation and so may represent actual geophysical structure (as noted in Khaykin et al., 2022).

4. Summary and Discussion

C2 data demonstrate that RO measurements are sensitive to the extremely large stratospheric H_2O perturbations during the first week following the HTHH eruption. This is tied to the large observed refractivity anomalies associated with the HTHH plume, combined with the low stratospheric background noise in the C2 measurements (with standard deviations of ~1% background values). Sensitivity calculations (Fig. 1) suggest that stratospheric H_2O anomalies of ~1000 ppmv or larger should be detectable in C2 refractivity measurements (equivalent to 3-sigma noise levels), with magnitude similar to a localized -8 K temperature anomaly.

To separate H_2O and temperature effects on *N* we have used independent temperature observations from the MLS satellite. This has some limitations in terms of different vertical sensitivities and imperfect co-locations between C2 and MLS measurements, but is a necessary step to separate H_2O and temperature influences on *N*. Comparison of MLS temperature anomalies vs. derived H_2O amount (Fig. 4) suggests small systematic temperature anomalies for the H_2O plume during the first week after the eruption, so that the C2 *N* anomalies are primarily due to H_2O influence. As noted above, we find similar results using ERA5 temperatures. In contrast, C2 dry temperature retrievals (atmPrf) for the anomalous HTHH profiles analyzed here show large negative temperature anomalies (up to -

20 K in Fig. 4), which are believed to mainly represent the response of dry temperature to H_2O. We note that Vömel et al (2022) identify small systematic temperature anomalies (~ -2K) associated with enhanced H_2O in the radiosonde measurements after January 29, possibly linked with radiative cooling from enhanced H_2O (Sellitto et al, 2022), but such patterns not detected in our MLS results (or ERA5 data) during the first week after the eruption.

Our simple H_2O retrieval shows maximum values of ~1500-2300 ppmv over the first few days following the eruption, over altitudes ~29-33 km. The H_2O magnitudes from the C2 retrieval are in reasonable agreement with radiosonde measurements over Australia, which cover altitudes up to ~30 km. MLS H_2O retrievals show somewhat smaller maximum values (~200-400 ppmv) over these days, but the MLS vertical sensitivity represents broader vertical layers (~3-4 km thick) that can underestimate the peak concentration and overestimate the vertical extent for narrow layers. Combining the H_2O sensitivity of RO with C2 background noise levels suggests that the C2 measurements are less sensitive to H_2O amounts below ~700 ppmv (equivalent to 2-sigma noise levels), so that C2 measurements are most useful for the large H_2O amounts in the first week after HTHH. Both radiosonde (Vömel et al, 2022) and MLS data (Millán et al, 2022) show that the HTHH plume disperses over time, with H_2O values <100 ppmv several weeks after the eruption. These smaller values, while highly anomalous and long-lasting in the stratosphere, are not retrievable from RO measurements.

Acknowledgements

The National Center for Atmospheric Research is sponsored by the U.S. National Science Foundation, and work in COSMIC is supported under the NSF-NASA Cooperative Agreement Grant 1522830. We thank the MLS group at the NASA Jet Propulsion Laboratory for helpful discussions, and we thank Rick Anthes for review and comments on the manuscript.

Data Availability Statement

The specially-processed COSMIC-2 data were obtained from the COSMIC Data Analysis and Archive Center (CDAAC) website https://data.cosmic.ucar.edu/gnss-ro/hthh_2022**.** Co-located ERA5 reanalysis temperatures were also obtained from the CDAAC website. MLS temperatures were obtained from the NASA EarthData website (https://search.earthdata.nasa.gov/search/granules?q=ML2H2O_004). The radiosonde H_2O profiles were obtained as described in Vömel et al., (2022) with data at https://gdex.ucar.edu/dataset/288_voemel.html.

References

Anthes, R.A., and Coauthors, 2008: The COSMIC/FORMOSAT-3 Mission: Early Results. *Bull. Am. Meteorol. Soc*., 89, 313–333, https://doi.org/10.1175/BAMS-89-3-313.

Hersbach, H., and coauthors (2020). The ERA5 global reanalysis. Quart. J. Roy. Meteor. Soc., https://doi.org/10.1002/qj.3803

Johnston, B. R., Randel, W. J., and Braun, J. J. (2022). Interannual Variability of Tropospheric Moisture and Temperature and Relationships to ENSO using COSMIC-1 GNSS-RO Retrievals. *Journal of Climate*, in press.

Khaykin, S., and coauthors (2022). Global perturbation of stratospheric water and aerosol burden by Hunga eruption. 30 August 2022, PREPRINT (Version 1) available at Research Square [https://doi.org/10.21203/rs.3.rs-1864748/v1], submitted to *Nature Geoscience.*

Kursinski, E. R., and coauthors (1997). Observing Earth's atmosphere with radio occultation measurements using the Global Positioning System. *J. Geophys. Res*., Vol. 102, No. 19, pp. 23,429-23,465.

Legras, B., and coauthors (2022). The evolution and dynamics of the Hunga Tonga plume in the stratosphere. E*GUsphere*, in review. https://doi.org/10.5194/egusphere-2022-517

Livesey, N. J., and coauthors (2018). Aura Microwave Limb Sounder (MLS) Version 4.2x level 2 and 3 data quality and description document. (Tech. Rep. No. JPL D-33509 Rev. D). Retrieved from http://mls.jpl.nasa.gov/

Millán, L., Santee, M. L., Lambert, A., Livesey, N. J., Werner, F., Schwartz, M. J., et al. (2022). The Hunga Tonga-Hunga Ha'apai Hydration of the Stratosphere. *Geophysical Research Letters*, *49*, e2022GL099381. https://doi.org/10.1029/2022GL099381

Sellitto, P., and coauthors (2022). The unexpected radiative impact of the Hunga Tonga eruption of January 15th, 2022. 18 April 2022, PREPRINT (Version 1) available at Research Square [https://doi.org/10.21203/rs.3.rs-1562573/v1], submitted to *Nature Geoscience*.

Smith, E. K., and S. Weintraub (1953). The Constants in the Equation for Atmospheric Refractive Index at Radio Frequencies. *Proceedings of the IRE*, **41**, 1035–1037, https://doi.org/10.1109/JRPROC.1953.274297.

Vömel, H., Evan, S., & Tully, M. (2022). Hunga Tonga-Hunga Ha'apai injects unprecedented amounts of water vapor into the stratosphere. *Science*, in press.

Xu, J., Li, D., Bai, Z., Tao, M. & Bian, J. (2022). Large Amounts of Water Vapor Were Injected into the Stratosphere by the Hunga Tonga–Hunga Ha'apai Volcano Eruption. *Atmosphere,* 13, 912. https://doi.org/10.3390/atmos13060912

Zeng, Z., and coauthors (2019). Representation of Vertical Atmospheric Structures by Radio Occultation Observations in the Upper Troposphere and Lower Stratosphere: Comparison to High Resolution Radiosonde Profiles. *J. Atmos. Ocean. Technol*., DOI:10.1175/JTECH-D-18-0105.1

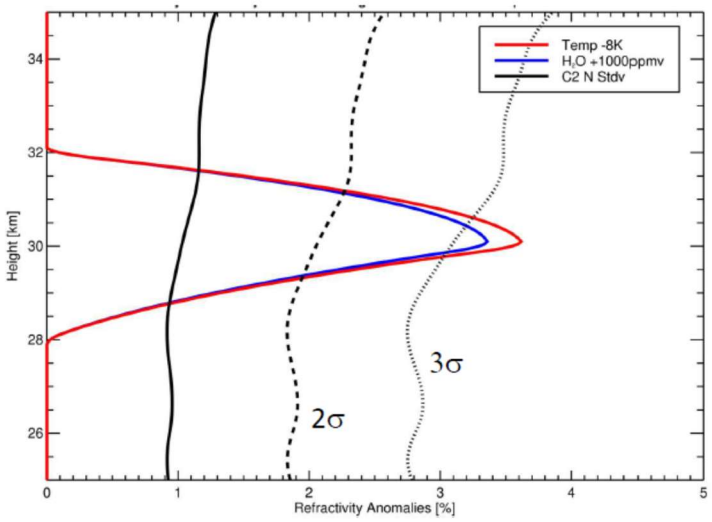

Figure 1. Vertical profiles of refractivity (N) anomalies associated with a localized 1000 ppmv H_2O perturbation at 30 km (blue) and a -8K temperature perturbation (red). Results are expressed in terms of percentage anomalies with respect to a standard background N profile. The solid black line shows the observed standard deviation (σ) for C2 N measurements based on non-volcanic conditions in the vicinity of HTHH, and the dashed and dotted lines show 2σ and 3σ values.

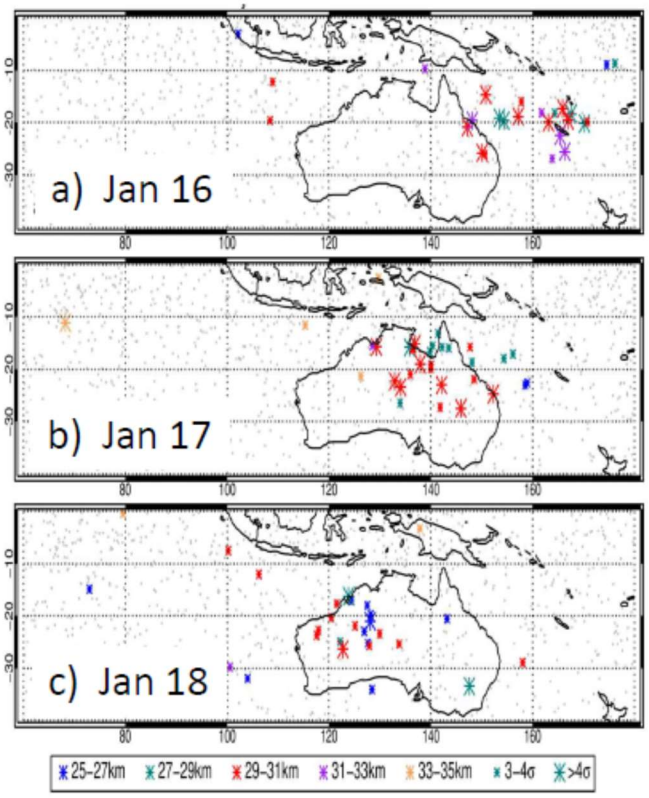

Figure 2. Grey dots show the C2 sounding locations in the region of the HTHH eruption on January 16, 17 and 18. Colored symbols indicate locations with positive N anomalies over altitudes 25-35 km exceeding 3-sigma background values, with color and size denoting the altitude and magnitude of the maximum N anomaly.

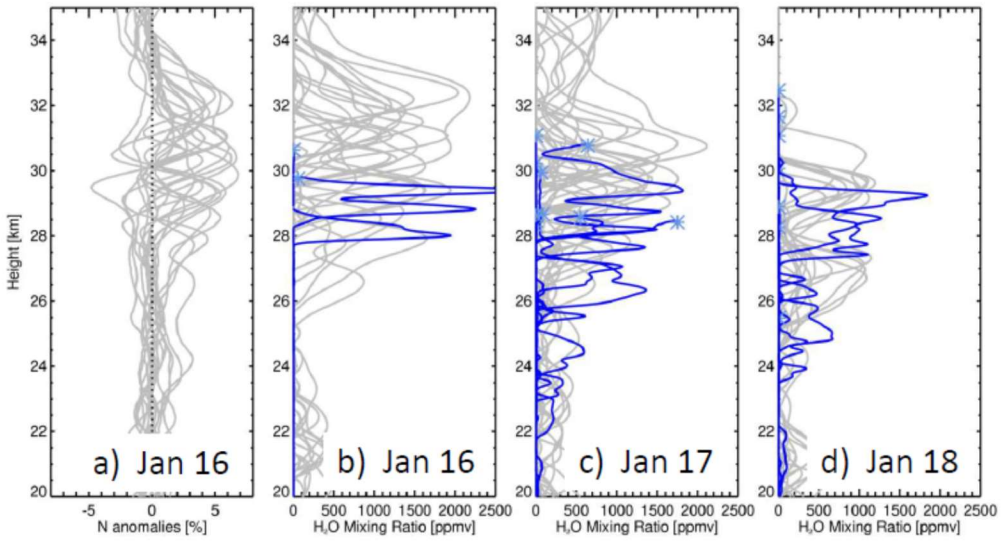

Figure 3. (a) Vertical profiles of refractivity (N) anomalies for cases selected on January 16 (colored symbols in Fig. 2a). (b-d) Vertical profiles of C2-derived H_2O mixing ratios (grey lines) for the cases selected on January 16-18 (colored symbols in Figs. 2a-c). The blue lines in (b-d) show radiosonde H_2O measurements over Australia during these days. Note that the radiosonde data only extend upwards to the balloon-burst altitude near ~30 km; the highest measurements in each profile are indicated by the blue asterisks.

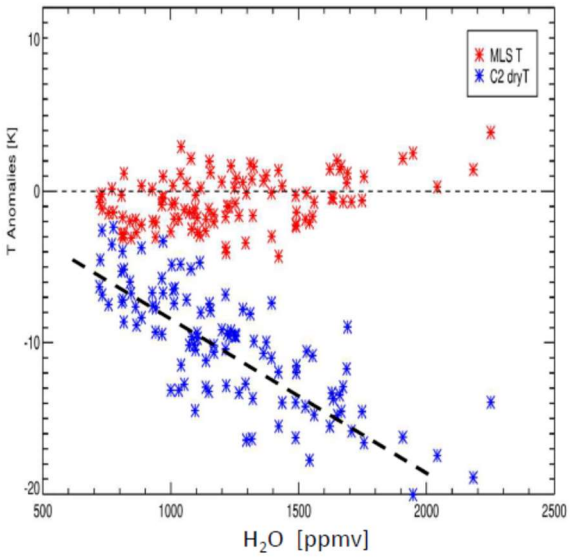

Figure 4. Red symbols show MLS temperature anomalies as a function of the C2 H_2O retrievals in the HTHH plume over January 16-18 (the same profiles as identified in Fig. 3). Blue symbols show the corresponding dry temperature anomalies calculated in the C2 dry retrievals (atmPrf). Black dashed line corresponds to a slope of (-8K/1000 ppmv), consistent with the T-H_2O sensitivity results shown in Fig. 1.

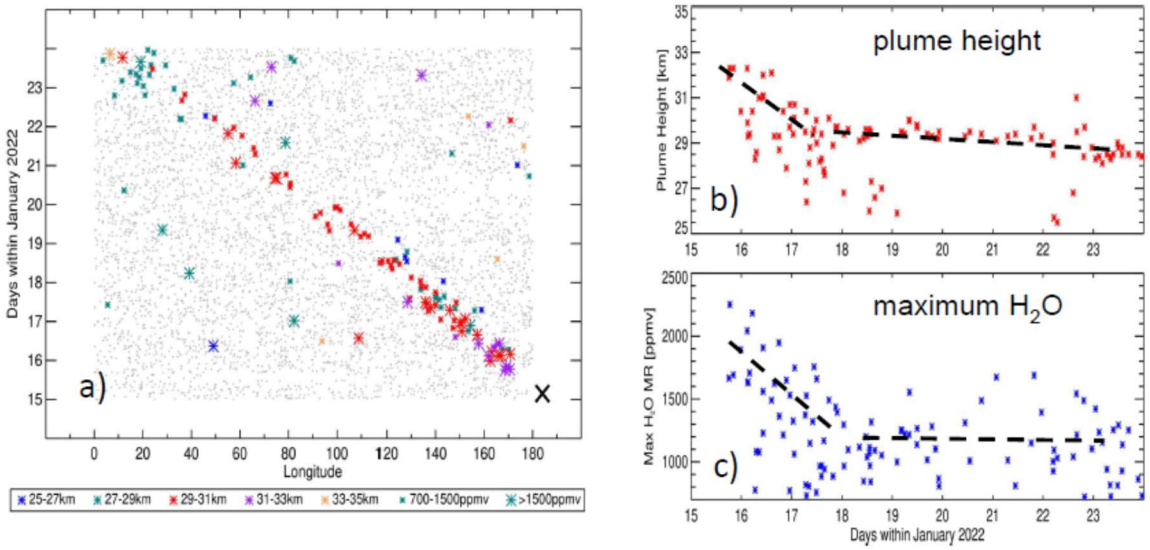

Figure 5. (a) Longitude vs. time diagram showing locations of H_2O profiles with maximum values >700 ppmv over 25-35 km, over the domain 10-30° S, for the first week following the HTHH eruption (noted by the 'X' on January 15). The colors and symbols denote the altitudes and magnitudes of the H_2O maxima. The grey dots indicate all of the C2 measurement locations. (b,c) Time series of plume height and H_2O maximum amount for C2 H_2O retrievals in the HTHH plume.

Supporting information for

Stratospheric water vapor from the Hunga Tonga – Hunga Ha'apai volcanic eruption deduced from COSMIC-2 radio occultation

William J. Randel[1,2], Benjamin R. Johnston[2], John J. Braun[2], Sergey Sokolovskiy[2], Holger Vömel[1], Aurelien Podglajen[3] and Bernard Legras[3]

[1] National Center for Atmospheric Research, Boulder, CO 80301

[2] COSMIC Program Office, University Corporation for Atmospheric Research, Boulder, CO 80301

[3] Laboratoire de Météorologie Dynamique (LMD-IPSL), UMR CNRS 8539, ENS-PSL, École Polytechnique, Sorbonne Université, Institut Pierre Simon Laplace, Paris, France

Contents of this file

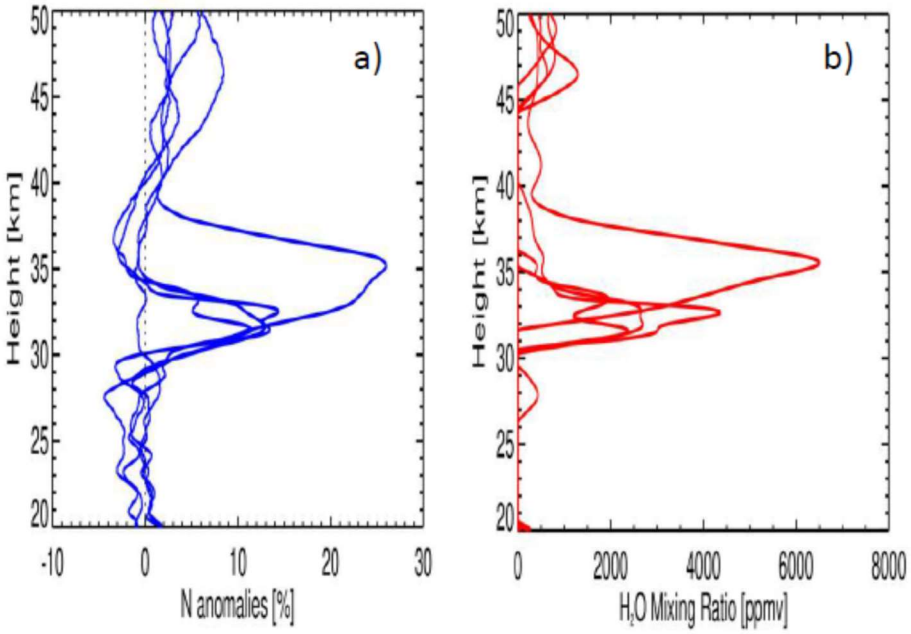

Figure S1. Vertical profiles of (a) refractivity anomaly and (b) derived H_2O mixing ratios for C2 observations within the HTHH plume on January 15. Most of these *N* profiles are associated with a 'bad' flag in the retrieval, although the structures are reasonable and may be consistent with actual geophysical information.